Blind Bi-Level Image Restoration With Iterated Quadratic Programming

Edmund Y. Lam, *Senior Member, IEEE*

***Abstract*—Many camera systems are dedicated to the capture of bi-level objects, including documents, bar codes, handwritten signatures, and vehicle license plates. Degradations in the imaging systems, however, cause blurring to the output images and introduce many more intensity levels. The blurring often arises from the optical aberrations and motions between the object and the camera, and hampers any computer vision algorithms aimed at automatic recognition and identification of these images. While image restoration has been applied frequently in such cases, many of these algorithms do not explicitly incorporate knowledge of a bi-level object, but attempt to apply a generic restoration scheme followed by thresholding. Such two-step algorithms may not produce the best results. On the other hand, directly restoring a bi-level object is a combinatorial task and is therefore time-consuming. In this brief, we propose a method that treats the blind restoration method as an iterated quadratic programming optimization problem. This has the properties of fast convergence and good numerical stability, due to established schemes such as the interior-point algorithm. The output of our algorithm is very nearly binary. Simulation results show that by integrating the computation in the imaging system, this proposed technique can restore weak signals that would have been lost with a simple thresholding.**

***Index Terms*—Bi-level images, blind deconvolution, image restoration, iteration, resolution enhancement.**

I. Introduction

MANY important objects are ideally bi-level or two-tone images. The most ubiquitous are documents, where black indicates text and white indicates background. In addition, we have line art, hand-written signatures, bar codes, and vehicle license plates, all of which are frequently handled by machine vision systems for automatic recognition and identification. The information contained in a bi-level image is often rich enough for such systems, while its relative simplicity permits much faster processing than its grayscale counterparts do. However, all imaging systems involve blurring and noise. These often arise from the aberrations in the optics and motions between the object and the camera, and the extent of such degradations may not be known to the system. The images at the sensor are no longer bi-level, and the algorithms cannot take advantage of the simplicity of bi-level as opposed to grayscale images. While a possible solution is to threshold the blurred images, some weak signals would be lost and the image quality will be deteriorated. A more rigorous treatment of this problem is therefore necessary.

Manuscript received October 18, 2005; revised July 10, 2006. This work was supported in part by the Research Grants Council of the Hong Kong Special Administrative Region, China under Project HKU 7164/03E. This paper was recommended by Associate Editor A. C. Kot.

The author is with the Department of Electrical and Electronic Engineering, University of Hong Kong, Hong Kong (e-mail: elam@eee.hku.hk).

Digital Object Identifier 10.1109/TCSII.2006.883101

The imaging process can be represented by

$$\begin{aligned} i(x,y) &= \sum_{j=-\infty}^{\infty} \sum_{k=-\infty}^{\infty} h(j,k) g(x-j, y-k) + n(x,y) \\ &= h(x,y) * g(x,y) + n(x,y) \end{aligned} \tag{1}$$

where $h(x,y)$ is the point-spread function, $g(x,y)$ is the object, $n(x,y)$ is the noise, and $i(x,y)$ is the captured image. For a diffraction-limited system under incoherent light, the point-spread function is a low-pass filter [1], and is often assumed to be spatially invariant. The observed image is therefore a noisy, blurred version of the object, with a lower resolution due to the filter. Digital post-processing is possible to restore the resolution content. In a classical problem formulation for image restoration, $h(x,y)$ is assumed to be known. Over the last thirty years, a multitude of techniques have been developed, and readers can consult references such as [2]–[5] for specific algorithms.

Our problem differs from the traditional image restoration framework on two grounds. First, the blur is unknown. The restoration problem without knowledge of the point-spread function is called blind deconvolution (when it is partially known, it is called semi-blind deconvolution [6]), which is known to be a much harder problem than image restoration [7]. Many diverse methods exist [8]: Algebraic methods treat the deconvolution problem as factorization of a bivariate polynomial, for which the absence of the fundamental theorem of algebra for higher dimensions suggests that the solution is almost always unique except for scaling and shifting [9], [10]. Projection-based methods treat the image and blur to be deterministic quantities, and seek an object that simultaneously satisfies a set of constraints [11]. Iterative schemes are employed in these methods [12]–[15]. Statistical methods assume certain distributions of the image and blur, and seek to maximize their probability through maximum likelihood (ML) or maximum *a posteriori* (MAP) techniques [8], [16]. Since deconvolution is an ill-posed problem, regularization is needed, and different norms such as l_2 norm and total-variation (TV) norm have also been applied to blind deconvolution [17]. Multichannel restoration has also been attempted [18].

Second, the intensity of the restored object can only take on two levels. Although it seems that the search space for possible solution is greatly reduced, the incorporation of this criterion as the prior information is very difficult [19]. For example, even if the restoration problem can be cast as a convex optimization problem with fast algorithms, the restriction to binary solutions destroys the convexity [20], [21]. The signal distribution also cannot be assumed Gaussian. Recent solutions mostly either restrict the design variables to a convex subset of the original feasible set [22], or relax the design variables to take on any

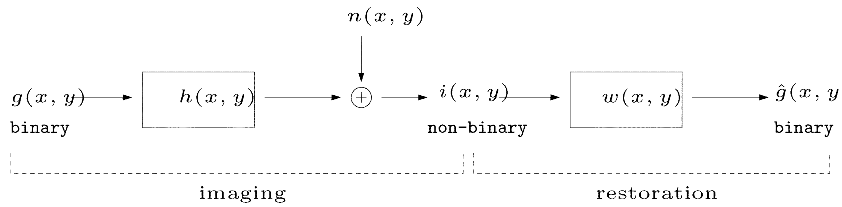

Fig. 1. Model for image restoration.

value between the binary intensities and then incorporate another procedure to push the intensity towards the extreme values [23]. In both cases, the techniques were developed for blind deconvolution of constant modulus signals, a common problem in communication channel equalization [24] and mathematically closely related to blind deconvolution. In recent years, there is also interest in developing specific blind deblurring methods for binary images, such as the iterative scheme in [25]. This algorithm employs a three-step iterative process, and each iteration uses gradient-descent schemes to arrive at the optimal point. Acknowledging this slow convergence, the authors of that paper suggested possible extensions using schemes such as conjugate gradient, simulated annealing, and genetic algorithms [25]. But the last two are also not fast techniques generally, and convergence can take a rather long time.

In this brief, we are motivated by the recent surge of interest in convex optimization techniques, which promise fast convergence and numerical stability such as with interior-point algorithms [20]. This can be applied to extend the work in [25] in deblurring bi-level images. However, as this problem is not convex in nature, in Section II we describe our formulation of the problem that makes use of convex optimization at its core. In particular, we will use quadratic programming as a special case of convex optimization. Like [25], the solution is also computed iteratively through a filtering process, but we will present a different formulation in putting the constraint of binary images. Simulation results are shown in Section III that demonstrate the effectiveness of our algorithm, with both 1-D data and images. Conclusions are drawn in Section IV.

II. Problem Formulation

Consider the linear filtering approach applied to the observed blurred image as shown in Fig. 1. The ideal criterion for the best design of the restoration filter $w(x,y)$ is that $\epsilon = E\left[(g(x,y) - \hat{g}(x,y))^2\right]$ is minimized. However, for blind deconvolution, we often seek a relaxed goal by requiring the output $\hat{g}(x,y)$ to satisfy certain *a priori* knowledge such as finite support and non-negativity [12], [14]. In our case, the prior knowledge is that $g(x,y)$ is binary, so we design the restoration filter $w(x,y)$ so that $\hat{g}(x,y)$ is also binary.

Another consideration is that even if $g(x,y)$ is binary, it can take on any two arbitrary values. In this brief, we assume that proper scaling and mean adjustment is possible, so that two values that the restored output $\hat{g}(x,y)$ should take on are ± 1. After the restoration process, we can display pixels with value $+1$ as black and pixels with value -1 as white, or vice versa. This can be trivially determined from the applications.

Because of these two ideal values of $\hat{g}(x,y)$, with a properly designed restoration filter we should have $[\hat{g}(x,y)]^2 - 1 \approx 0$ for all values of x and y. We can then set up the optimization problem as follows:

$$\begin{aligned} \text{minimize} \quad & \|t(x,y)\|^2 \\ \text{subject to} \quad & -t(x,y) \preceq [w(x,y) * i(x,y)] \\ & \bullet [w(x,y) * i(x,y)] - \mathbf{1} \preceq t(x,y) \end{aligned} \tag{2}$$

where the symbol $\preceq$ denotes element-by-element comparison and $\bullet$ denotes element-by-element multiplication. Note that $t(x,y)$'s are auxillary variables that help us convert the problem to a standard form at a later stage. A small value of $\|t(x,y)\|^2$ is achieved if and only if $|[w(x,y) * i(x,y)] \bullet [w(x,y) * i(x,y)]| - 1 \approx 0$, i.e., $\hat{g}(x,y) \approx \pm 1$ for all (x,y). Solving this optimization problem would effectively tune $w(x,y)$ to produce binary outputs [26].

It should be remarked, though, that the constraints in (2) are not convex [20]. There is no direct algorithm to find the global optimal solution. Instead, as with [14], a recursive filtering technique is used. This is schematically depicted in Fig. 2. Here, we explain the algorithm in details.

1) First, let k denote the current number of iterations. At the beginning, set $k = 0$.
2) Second, make an estimate of $w^{(k)}(x,y)$, where the superscript denotes the iteration number. Without further information at this point, we use a simple high-pass filter for $w^{(k)}(x,y)$ (such as a Laplacian, in the absence of information about $h(x,y)$) because $h(x,y)$ is a low-pass filter. We can then compute

$$\hat{g}^{(k)}(x,y) = w^{(k)}(x,y) * i(x,y). \tag{3}$$

3) Third, we set up the optimization problem

$$\begin{aligned} \text{minimize} \quad & \|t(x,y)\|^2 \\ \text{subject to} \quad & -t(x,y) \preceq [\hat{g}^{(k)}(x,y)] \\ & \bullet [w(x,y) * i(x,y)] - 1 \preceq t(x,y). \end{aligned} \tag{4}$$

Comparing (4) and (3), we can see that we have replaced one of the $w(x,y)$'s by $w^{(k)}(x,y)$, making the problem now linear in $w(x,y)$. If the iteration converges, $w^{(k)}(x,y)$ should be a good estimate of $w(x,y)$ and this new optimization problem will become similar to our original problem in (3). We have not yet proved convergence, although preliminary experiments seem to corroborate this claim.

If we use the l_2 norm in the objective function, the above can be converted to a quadratic programming as follows [23]: let $\mathbf{w}$ be the raster-scan of $w(x,y)$, $\mathbf{t}$ be the raster-scan of $t(x,y)$, and $\hat{G}^{(k)}$ be a diagonal matrix whose diagonal entries are $\hat{g}^{(k)}(x,y)$. If the images are of size $M \times M$, and the restoration filter has size $N \times N$, then $\mathbf{w}$ is a vector of length N^2, $\mathbf{t}$ a vector of length M^2, and $\hat{G}^{(k)}$ a matrix of size $M^2 \times M^2$. Furthermore, let $\mathcal{I}$ be an $M^2 \times N^2$ matrix built from the data in $i(x,y)$ such that $\mathcal{I}\mathbf{w}$ would be the raster-scan of $w(x,y) * i(x,y)$. We also construct a new variable $\phi = [\mathbf{w};\ \mathbf{t}]^T$.

Optimization problem (4) can be recasted as

$$\begin{aligned} &\text{minimize} \quad \phi^T P \phi \\ &\text{subject to} \quad -\mathbf{t} \preceq \hat{G}^{(k)} \mathcal{I}\mathbf{w} - \mathbf{1} \preceq \mathbf{t} \end{aligned} \tag{5}$$

where

$$P = \begin{bmatrix} 0 & 0 \\ 0 & I \end{bmatrix} \tag{6}$$

has zero entries except at the lower right corner, which has an $M^2 \times M^2$ identity matrix. The objective function is therefore quadratic in ϕ. We can further rearrange the terms of the constraints in (5) to

$$\begin{bmatrix} -\hat{G}^{(k)}\mathcal{I} & -I \end{bmatrix} \begin{bmatrix} \mathbf{w} \\ \mathbf{t} \end{bmatrix} \preceq -\mathbf{1} \tag{7}$$

$$\begin{bmatrix} \hat{G}^{(k)}\mathcal{I} & -I \end{bmatrix} \begin{bmatrix} \mathbf{w} \\ \mathbf{t} \end{bmatrix} \preceq \mathbf{1}. \tag{8}$$

These constraints are affine in ϕ. Therefore, the optimization problem can be solved via quadratic programming. The logarithmic barrier method can be constructed as follows: Let a_i^T be the ith row of $[\,-\hat{G}^{(k)}\mathcal{I} \quad -I\,]$ and b_i^T be the ith row of $[\,\hat{G}^{(k)}\mathcal{I} \quad -I\,]$, where i extends from 1 to M^2. The inequalities

$$a_i^T \phi + 1 \leq 0 \tag{9}$$

$$b_i^T \phi - 1 \leq 0 \tag{10}$$

for $1 \leq i \leq M^2$ are therefore the same as (7) and (8). We still have a constrained minimization problem to solve; but instead of directly approaching it, we can form an unconstrained optimization problem by minimizing

$$\phi^T P \phi - \frac{1}{\mu} \sum_{i=1}^{M^2} \left[\log(-a_i^T \phi - 1) + \log(-b_i^T \phi + 1) \right] \tag{11}$$

where μ is a positive number. The logarithm terms act as barriers to ensure that the arguments within them must be positive, and the larger the value of μ, the stronger the barriers [20]. Since this objective function is convex in ϕ, it can be solved efficiently using methods such as Newton. However, if μ is large, the Hessian varies rapidly near the boundary of the feasible set and makes the Newton iterations difficult numerically. Therefore, the recommended steps are to solve (11) iteratively and increase μ at each step, starting the Newton iteration from the solution of the previous one. For other alternatives in solving quadratic programming, such as the primal-dual interior-point method, the reader can consult [27].

4) Fourth, we compute $\tilde{w}(x,y) = [I \quad 0]\phi$. Note that $\tilde{w}(x,y)$ is not yet the optimal solution, because it produces nearly binary signals only together with (3). Therefore, this result should be used to fine-tune for the next estimate of $w^{(k+1)}(x,y)$, as depicted in Fig. 2, with

$$w^{(k+1)}(x,y) = \lambda w^{(k)}(x,y) + (1-\lambda)\tilde{w}(x,y) \tag{12}$$

where $0 < \lambda < 1$ [23].

5) Fifth, we go back to step (2) with this new estimate, and increment the value of k by one. If the values of $\hat{g}^{(k)}(x,y)$ at that stage are already binary or very close to be, we will terminate the looping and return $\hat{g}^{(k)}(x,y)$ as the restored image. Otherwise, we will proceed within the loop.

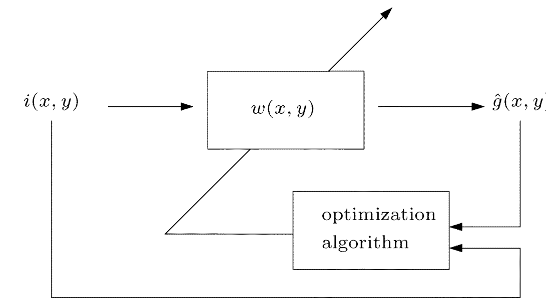

Fig. 2. Model for recursive image filtering.

III. Simulation

We apply the algorithm described above to the blind restoration of several bi-level images. To demonstrate the effect of the algorithm, we first consider a one-dimension example, which can be considered a horizontal scan of a bar code [28] as depicted in Fig. 3.At the 15th position, there is a singular pixel occupying the value -1 while its neighbors take the value $+1$. When this image is blurred by a simple averaging filter (i.e., $h = [1 \quad 1 \quad 1]/3$) as shown in (c), the sharp transitions become more gradual. Moreover, the intensity at the 15th position is now positive. If we simply apply thresholding at this stage, the singular intensity value would be lost. Fine details would not be preserved. On the other hand, if we apply the iterative deconvolution scheme described in this brief, the results are shown in (d) (with five iterations) and (e) (with ten iterations). In both cases, we can observe that the singular value at the 15th position is now restored to a negative value. If we perform thresholding (setting the threshold at zero) after the image restoration, we would correctly recover its intensity. Using more iterations is seen to increase the margin between the threshold value and the restored value at the singular point. This is very desirable to withstand the effect of noise.

We also show, in Fig. 4, a plot of the value of the cost function in (5) with respect to the number of iterations. We perform the simulation with λ in (12) ranging from 0.5 to 0.95. In each iteration, the vertical bar covers the range of values within plus or minus one standard deviation when different values for λ are used. Note that iteration 0 refers to the cost function before any optimization, and iteration 1 refers to the result of the first optimization, both of which are unaffected by the choice of λ. We can see that the optimization functional forms a decreasing sequence with respect to the number of iterations. This indicates that the restored values are approaching ± 1, affirming that the resulting images after restoration are closer to binary.

An example of restoration of a 2-D image is shown in Fig. 5. The original text image of size 256×100 depicted in (a) takes on only two possible intensity values, visually displayed as black and white. It then undergoes a motion blur and added with some Gaussian noise to give the image in (b). Shades of gray appear as a result of the blurring. Even though we can still read the letters, if we subject the image to a simple

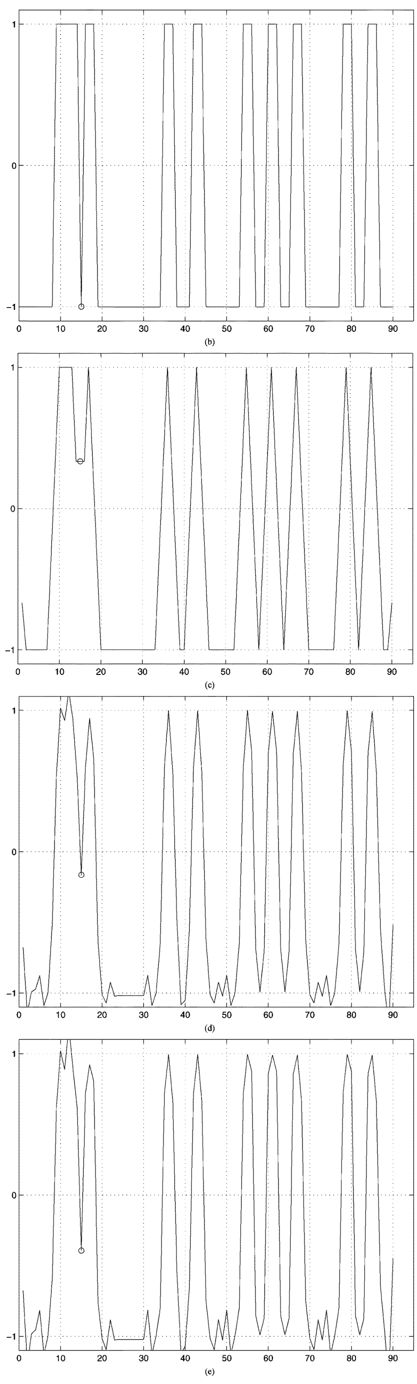

Fig. 3. Blind deconvolution of binary (1-D) images with the proposed scheme. (a) Original image. (b) Blurred image. (c) After five iterations. (d) After 10 iterations.

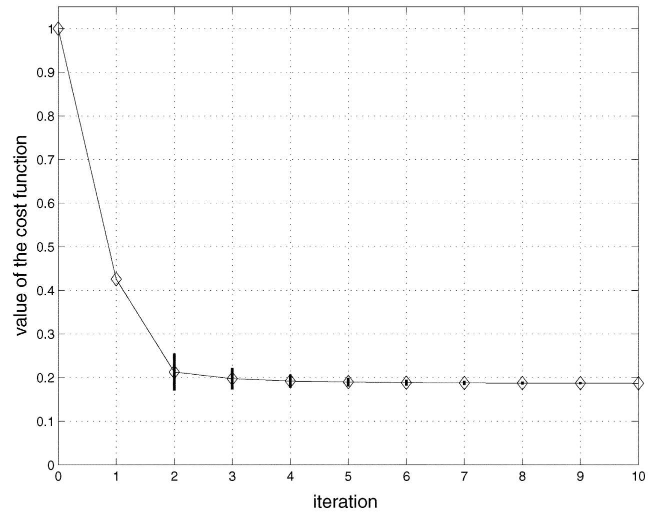

Fig. 4. Value of the optimization functional with respect to the iterations.

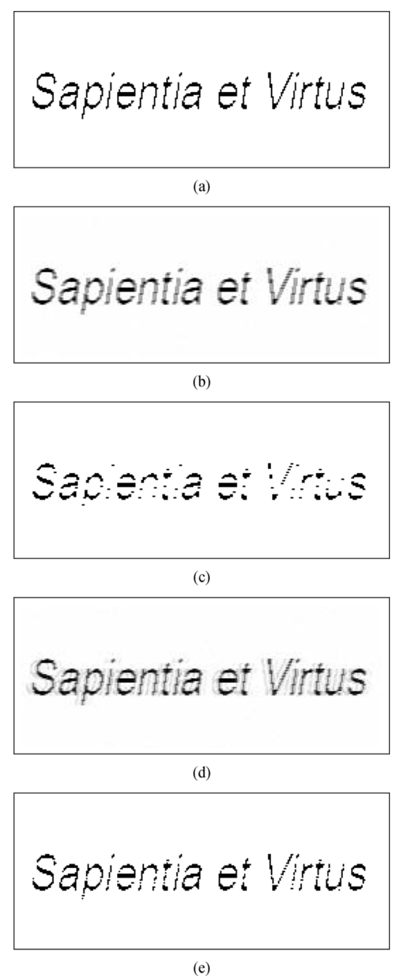

Fig. 5. Blind deconvolution of a binary (2-D) image with the proposed scheme. (a) Original image. (b) Blurred and noisy image. (c) With simple thresholding. (d) After 10 iterations. (e) After thresholding.

thresholding operation, we will obtain the image in (c). Fine details are lost, and the image makes it hard for tasks such as pattern recognition or optical character recognition. However, if we apply the blind deconvolution algorithm to the image in (b), after 10 iterations we obtain the restored image as shown in (d). The restored image evidently has increased high frequency information, which after thresholding would return a rather readable set of characters, as shown in (e). Similarly, we show an example of a binarized map in Fig. 6 that has undergone a 5×5 Gaussian blur to simulate defocus. As in the previous case, random noise has also been added. Simple thresholding of the blurred and noisy image again would render some texts unreadable, while adding the restoration step before thresholding improves the result.

Fig. 6. Restoration of a binary image with Gaussian blur. (a) Blurred and noisy image. (b) With simple thresholding. (c) After restoration and thresholding.

IV. Summary and Conclusion

In this brief, we have described a novel blind image deconvolution method for restoring binary images. The prior knowledge of a binary source is embedded in an optimization formulation, which is tackled with an iterative quadratic programming algorithm. Our preliminary results show that this method is capable of restoring blurred images, which makes it suitable for machine vision tasks such as pattern recognition. Further investigations will focus on the issues of convergence and numerical stability, as well as more extensive testing and fine-tuning of the algorithm for images corrupted with more severe blurs.

References

[1] J. W. Goodman, *Introduction to Fourier Optics*, third ed. Colorado city, CO: Roberts and Company, 2004.

[2] H. Andrews and B. Hunt, *Digital Image Restoration*. Englewood Cliffs, NJ: Prentice-Hall, 1977.

[3] H. Stark, Ed., Image Recovery: Theory and Application New York, Academic, 1987.

[4] A. K. Katsaggelos, *Digital Image Restoration*. New York: Springer-Verlag, 1991.

[5] R. C. Gonzalez and R. E. Woods, *Digital Image Processing*, second ed. Englewood Cliffs, NJ: Prentice-Hall, 2002.

[6] L. Bar, N. Sochen, and N. Kiryati, "Semi-blind image restoration via Mumford-Shah regularization," *IEEE Trans. Image Process.*, vol. 15, no. 2, pp. 483–493, Feb. 2006.

[7] D. Kundur and D. Hatzinakos, "Blind image deconvolution," *IEEE Signal Process. Mag.*, vol. 13, no. 5, pp. 43–64, May 1996.

[8] E. Y. Lam and J. W. Goodman, "An iterative statistical approach to blind image deconvolution," *J. Opt. Soc. Amer. A*, vol. 17, no. 7, pp. 1177–1184, Jul. 2000.

[9] R. H. T. Bates, B. K. Quek, and C. R. Parker, "Some implications of zero sheets for blind deconvolution and phase retrieval," *J. Opt. Soc. Amer. A* , vol. 7, no. 3, pp. 468–479, Mar. 1990.

[10] D. C. Ghiglia, L. A. Romero, and G. A. Mastin, "Systematic approach to two-dimensional blind deconvolution by zero-sheet separation," *J. Opt. Soc. Amer. A* , vol. 10, no. 5, pp. 1024–1036, May 1993.

[11] H. Stark and Y. Yang, *Vector Space Projections: A Numerical Approach to Signal and Image Processing, Neural Nets, and Optics*. New York: Wiley, 1998.

[12] G. R. Ayers and J. C. Dainty, "Iterative blind deconvolution method and its applications," *Opt. Lett.*, vol. 13, no. 7, pp. 547–549, Jul. 1988.

[13] Y.-L. You and M. Kaveh, "A regularization approach to joint blur identification and image restoration," *IEEE Trans. Image Process.*, vol. 5, no. 3, pp. 416–428, Mar. 1996.

[14] D. Kundur and D. Hatzinakos, "A novel blind deconvolution scheme for image restoration using recursive filtering," *IEEE Trans. Signal Process.*, vol. 46, no. 2, pp. 375–390, Feb. 1998.

[15] E. Y. Lam and J. W. Goodman, N. Sampat and T. Yeh, Eds., "Iterative blind image deconvolution in space and frequency domains," in *Proc. SPIE Sensors, Cameras, Appl. for Digital Photography*, Jan. 1999, vol. 3650, pp. 70–77.

[16] K.-T. Lay and A. K. Katsaggelos, "Image identification and restoration based on the expectation-maximization algorithm," *Opt. Eng.*, vol. 29, no. 5, pp. 436–446, May 1990.

[17] T. Chan and C.-K. Wong, "Total variation blind deconvolution," *IEEE Trans. Image Process.*, vol. 7, no. 3, pp. 370–375, Mar. 1998.

[18] G. Panci, P. Campisi, S. Colonnese, and G. Scarano, "Multichannel blind image deconvolution using the bussgang algorithm: Spatial and multiresolution approaches," *IEEE Trans. Image Process.*, vol. 12, no. 11, pp. 1324–1337, Nov. 2003.

[19] J. Keuchel, C. Schnörr, C. Schellewald, and D. Cremers, "Binary partitioning, perceptual grouping, and restoration with semidefinite programming," *IEEE Trans. Pattern Anal. Machine Intell.*, vol. 25, no. 11, pp. 1364–1379, Nov. 2003.

[20] S. Boyd and L. Vandenberghe, *Convex Optimization*. Cambridge, U.K.: Cambridge Univ. Press, 2004.

[21] T. F. Chan, S. Esedoglu, and M. Nikolova, "Finding the global minimum for binary image restoration," in *Proc. 2005 IEEE Int. Conf. Image Process.*, 2005, vol. 1, pp. 121–124.

[22] B. Maricić, Z.-Q. Luo, and T. N. Davidson, "Blind equalization of constant modulus signals via restricted convex optimization," in *Proc. 2001 IEEE Int. Conf. Acoust., Speech, Signal Process.*, 2001, vol. 4, pp. 2169–2172.

[23] I. Santamaría, C. Pantaleón, L. Vielva, and J. Ibáñez, "Blind equalization of constant modulus signals using support vector machines," *IEEE Trans. Signal Process.*, vol. 52, no. 6, pp. 1773–1782, Jun. 2004.

[24] M. Kawamoto, M. Ohata, K. Kohno, Y. Inouye, and A. K. Nandi, "Robust super-exponential methods for blind equalization in the presence of Gaussian noise," *IEEE Trans. Circuits Syst. II, Exp. Briefs*, vol. 52, no. 10, pp. 651–655, Oct. 2005.

[25] T.-H. Li and K.-S. Lii, "A joint estimation approach for two-tone image deblurring by blind deconvolution," *IEEE Trans. Image Process.*, vol. 11, no. 8, pp. 847–858, Aug. 2002.

[26] E. Y. Lam, "Blind deconvolution of bi-level images with successive filtering," in *Proc. 20th Congress Int. Commission Optics*, Aug. 2005, pp. 1228–1233.

[27] A. Forsgren, P. E. Gill, and M. H. Wright, "Interior methods for nonlinear optimization," *SIAM Rev.*, vol. 44, no. 4, pp. 525–597, 2002.

[28] S. Esedoglu, "Blind deconvolution of bar code signals," *Inv. Prob.*, vol. 20, pp. 121–135, 2004.